Available online at www.sciencedirect.com
ScienceDirect
Coordination Chemistry Reviews 251 (2007) 1822–1833
COORDINATION CHEMISTRY REVIEWS
www.elsevier.com/locate/ccr

Review

Spin crossover and photomagnetism in dinuclear iron(II) compounds☆

Azzedine Bousseksou[a,*], Gábor Molnár[a], José Antonio Real[b], Koichiro Tanaka[c]

[a] *Laboratoire de Chimie de Coordination, CNRS UPR-8241, 205 route de Narbonne, 31077 Toulouse, France*
[b] *Instituto de Ciencia Molecular, Dep. Química Inorgánica, Universidad de Valencia, 46071 Valencia, Spain*
[c] *Department of Physics, Graduate School of Science, Kyoto University, Sakyo, Kyoto 606-8502, Japan*

Received 31 October 2006; accepted 26 February 2007
Available online 2 March 2007

Contents

Abstract

In this paper, we review recent work reported in the field of molecular spin crossover phenomena in dinuclear compounds. Following a comprehensive overview on the synthesis and properties of new iron(II) dinuclear compounds presenting the spin crossover phenomenon, we focus this review on recent efforts made in studying and understanding the photo-physical properties of the $\{[Fe(L)(NCX)_2]_2bpym\}$ (L = bt or bpym, X = S or Se) family of compounds. Finally, literature on the different theoretical approaches treating the static and dynamic properties of dinuclear complexes presenting two-step thermal spin transition is briefly summarized.

Keywords: Spin crossover; Dinuclear complexes; LIESST effect; Ising-like model

1. New dinuclear iron(II) spin crossover compounds

Examples of dinuclear SCO compounds reported until recently were only based on bpym-bridged iron(II) compounds [1]. Interestingly, both the spin state and magnetic coupling exhibited by them can be switched by the action of temperature, pressure or light and involve the occurrence of the following three spin-pair state transformations LS–LS ↔ LS–HS ↔ HS–HS (where LS and HS represent the local low-spin and high-spin states, respectively, of the dinuclear species). This singular switchable behavior and the possibility to extend this phenomenology to other polynuclear compounds have attracted the attention of several research groups working in the field. In this respect, a series of new dinuclear iron(II) SCO compounds, reported by the groups of Murray, Brooker, Kaizaki and Real among others, have added new interesting results to this topic. Such investigations have confirmed the occurrence of two-step transitions but also single step transitions, which suggest the occurrence of two different SCO processes, namely LS–LS ↔ LS–HS ↔ HS–HS and LS–LS ↔ HS–HS. Further-

Abbreviations: 4,4′-bipy, 4,4′-bipyridine; bpym, 2,2′-bipyrimidine; bpypz, 3,5-bis(2-pyridyl)-pyrazole; bt, 2,2′-bithiazoline; bztpen, *N*-benzyl-*N*,*N*′,*N*′-tris(2-pyridylmethyl)ethylene-diamine; dpa, dipyridylamine; HS, high spin; LIESST, light induced excited spin state trapping; LS, low spin; phdia, 4,7-phenanthroline-5,6-diamine; 4-phpy, 4-phenylpyridine; pmat, *N*-(2-pyridylmethyl)4-amino-5-(2-pyridylmethylaminomethyl)4*H*-l,2,4-triazol-3-ylmeth anamine; ptz, 1-propyltetrazole; py, pyridine; 2-pic, 2-picolylamine; pypzH, 2-pyrazolylpyridine; SCO, spin crossover; tpa, tris(2-pyridylmethyl) amine

☆ Based on a keynote lecture presented at the 37th International Conference on Coordination Chemistry, 13–18 August 2006, Cape Town, South Africa.

* Corresponding author. Tel.: +33 561333153; fax: +33 561553003.
E-mail address: boussek@lcc-toulouse.fr (A. Bousseksou).

0010-8545/$ – see front matter © 2007 Elsevier B.V. All rights reserved.
doi:10.1016/j.ccr.2007.02.023

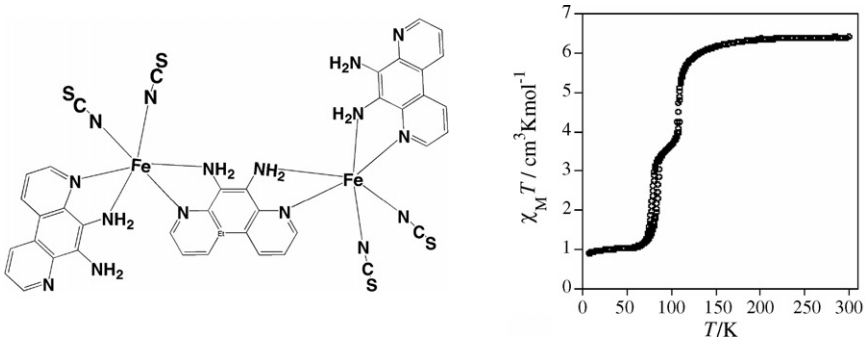

Fig. 1. Proposed structure and magnetic behavior of $\{[Fe(phdia)(NCS)_2]_2(phdia)\}$ [2].

more, in the case of two-step spin transitions, it has been demonstrated that the plateau observed between the two separate transitions can be associated with existence of the mixed LS–HS spin state, or with a 1:1 mixture of HS–HS and LS–LS states. In the following, we illustrate the most representative dinuclear compounds synthesized in the last years.

The compound $\{[Fe(phdia)(NCS)_2]_2(phdia)\}$ (see Fig. 1 left) exhibits a two-step spin transition, with $T_{c1} = 108$ K and $T_{c2} = 80$ K, displaying 2 K and 7 K wide thermal hysteresis loops in the upper and the lower steps, respectively (Fig. 1 right) [2]. A plateau of ca. 20 K width centered at ca. 90 K, which corresponds to the 50% of the spin conversion, separates the two transitions. Using Mössbauer spectroscopy in an external magnetic field, the composition of the plateau was identified in the metastable state after quenching it to 4.2 K. Such experiments demonstrated that the plateau consists mainly of LS–HS pairs and confirmed the hypothesis that the spin conversion in several dinuclear Fe(II) entities proceeds following the sequence LS–LS ↔ LS–HS ↔ HS–HS. Moreover, LIESST experiments performed on this compound revealed, as in $\{[Fe(bt)(NCS)_2]_2bpym\}$ [3], that the photo-induced species corresponds to LS–HS pairs, which is a further evidence of the inherent stability of the mixed spin state. These observations are in agreement with the DFT calculations on the energetics of dinuclear bpym-bridged spin transition complexes as well [4].

Dinuclear complexes with formula $\{[Fe(bztpen)]_2[\mu\text{-}N(CN)_2]\}(PF_6)_3 \cdot nH_2O$ ($n = 1, 0$) have been recently synthesized by Real et al. [5]. In these complexes each iron(II) atom presents a distorted $[FeN_6]$ octahedral coordination defined by the pentadentate ligand and a bridging dicyanamide ligand (Fig. 2 left). Depending on the form and history of the sample, the monohydrated compound exhibits a paramagnetic behavior (single crystals) or displays a very incomplete spin transition at 0.01 GPa, which disappears after several cooling–warming cycles (precipitated microcrystalline sample). This monohydrate form undergoes a 50% spin transition at ca. 0.32 GPa, which presumably, follows the HS–HS ↔ HS–LS transformation. The anhydrous form shows a gradual two-step spin transition with no observed hysteresis in the solid state. Both steps are approximately 100 K wide, centered at ≈200 K and ≈350 K, with a plateau of approximately 80 K separating the transitions (Fig. 2 right). Its crystal structure has been determined in steps of approximately 50 K between 400 K and 90 K, which provided a deeper insight into the structural behavior in a complex exhibiting two-step transition. Two crystallographically distinct dinuclear molecules have been identified in the crystal. As a consequence, the step-wise nature of the spin transition could be assumed to be associated with this fact. However, the multi-temperature X-ray study has demonstrated that the two molecules undergo SCO simultaneously. At the plateau, the structural and magnetic data indicate that the intermediate state is half way between the high and low spin states, most likely consisting of HS–LS pairs. The SCO behavior of the anhydrous form has also been studied in solution ([d^6] acetone) by the Evans method. In solution, this compound undergoes a continuous decrease in $\chi_M T$ without the characteristic plateau.

The compound $\{[Fe_2(pmat)_2](BF_4)_4 \cdot DMF\}$ reported by Brooker and Murray and co-workers has provided the oppor-

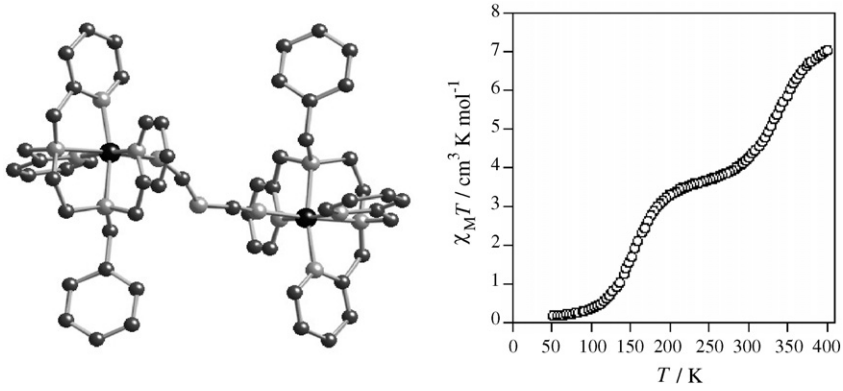

Fig. 2. Molecular structure and magnetic properties in the solid state of the complex $\{[Fe(bztpen)]_2[\mu\text{-}N(CN)_2]\}(PF_6)_3$ [5].

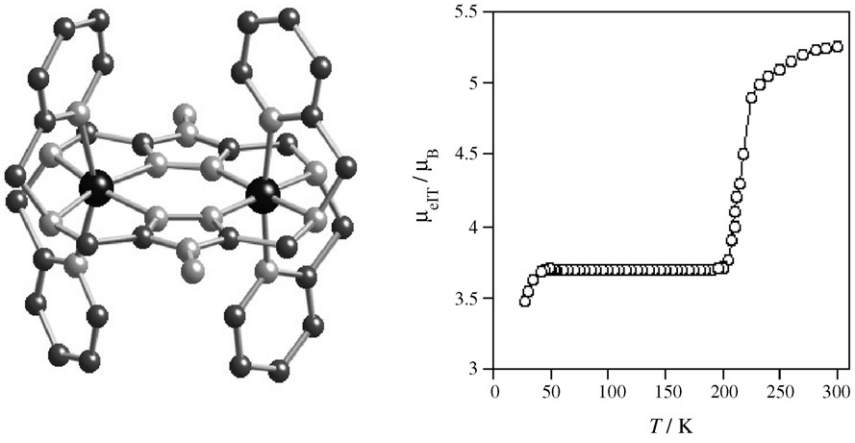

Fig. 3. Molecular structure and magnetic properties of the complex $\{[Fe_2(pmat)_2](BF_4)_4{\cdot}DMF\}$. Adapted from Ref. [6]. Reproduced by permission of the Royal Society of Chemistry.

tunity to characterize the mixed LS–HS spin state by X-ray crystallography [6]. At ambient pressure and in the temperature range of 300–4 K only the first step, HS–HS ↔ LS–HS, of a possible two-step transition is accomplished in this system (Fig. 3 right). This 50% transition is abrupt and occurs at $T_c = 224$ K. Similar SCO behavior has been reported for $\{[Fe(bt)(NCSe)_2]_2bpym\}$ [7a] and $\{[Fe(bpym)(NCS)_2]_2bpym\}$ [7b], at atmospheric pressure and at 0.1 GPa, respectively. Each iron(II) center defines a distorted octahedral coordination environment made up of three donor atoms from each of the two pmat ligands, which sandwich the two metal centers (Fig. 3). In the equatorial plane the iron atoms are bridged by the 1,2,4-triazole moieties. At 293 K, the unit cell contains one half of the dinuclear complex while the other half is generated by a center of inversion. The Fe–N bond lengths are in the range of 2.116(4)–2.303(5) Å and consistent with those expected for HS iron(II) ions. The crystal data at 123 K show that the unit cell contains the entire complex, the two iron(II) atoms being crystallographically independent. The spin states are unambiguously assigned to Fe(1) being LS [Fe–N: 1.934(3)–2.071(4) Å, *cis* N–Fe–N angles 81.8(1)–101.1(2)°] and Fe(2) being HS [Fe–N: 2.131(3)–2.319(4) Å, *cis* N–Fe–N angles 75.1(1)–121.7(1)°]. Most probably, the second step LS–HS ↔ LS–LS could be observed under applied hydrostatic pressure.

The tetranuclear complex $\{[Fe_4(\mu\text{-}CN)_4(bpy)_4(tpa)_2](PF_6)_4\}$ with square geometry (Fig. 4 right), first reported by Vahrenkamp et al. [8], has recently been reinvestigated by Oshio and co-workers [9]. Temperature dependence of magnetic susceptibility (Fig. 4 left) and Mössbauer spectra showed that despite its tetranuclear nature this compound behaves like a two-step SCO dinuclear system. In the squares, both $\{[Fe(bpy)_2]^{2+}\}$ and $\{[Fe(tpa)_2]^{2+}\}$ centers are alternately bridged by four CN^- groups with the carbon atoms coordinated to the Fe(II) ions of the $\{[Fe(bpy)_2]^{2+}\}$ centers, which remain permanently in the LS state. The temperature dependence of the magnetic susceptibility over the range of 2–400 K clearly denotes a two-step spin transition with a plateau of approximately 100 K centered at around 240 K. The structure shows the Fe(II) ions are LS below 100 K (average coordination bond lengths: 1.958 Å for $\{[Fe(bpy)_2]^{2+}\}$ and 1.976 Å $\{[Fe(tpa)_2]^{2+}\}$). At 200 K, one $\{[Fe(tpa)_2]^{2+}\}$ center becomes HS showing longer bonds to the ligands ranging from 2.154 Å to 2.165 Å. Above 300 K the onset of a second transition, not characterized crystallographically, appears. Certainly, the plateau observed between 200 K and 300 K corresponds to a mixed LS–HS spin configuration of the $\{[Fe(tpa)_2](\mu\text{-}NC)_2\}$ centers.

Thermal spin crossover in the binuclear iron(II) helicate $[Fe_2(5\text{-bismbmp})]^{4+}$ (5-bismbmp = bis[5-(l-metbyl-2-(5′-

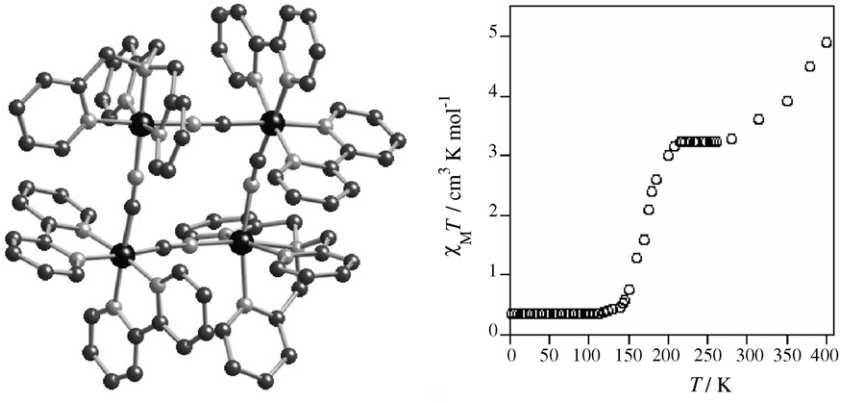

Fig. 4. Molecular structure and magnetic properties of the complex $\{[Fe_4(\mu\text{-}CN)_4(bpy)_4(tpa)_2](PF_6)_4\}$ [9].

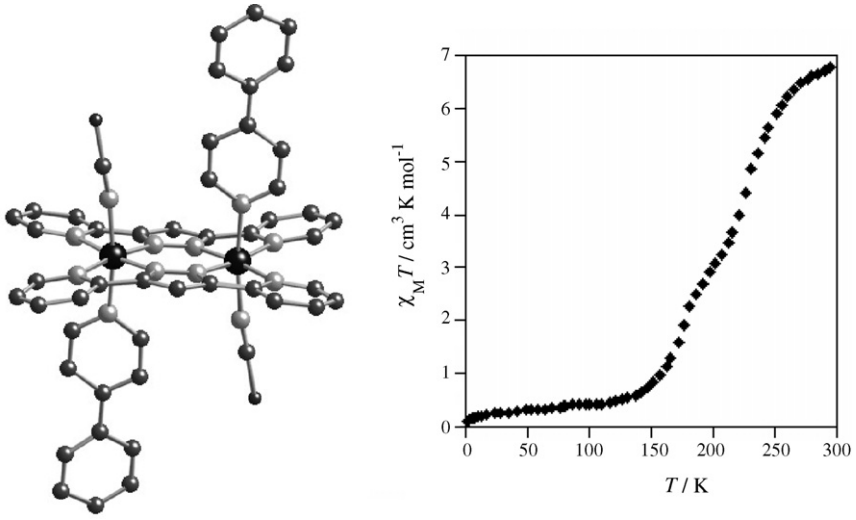

Fig. 5. Molecular structure and magnetic properties of the complex $\{[Fe(NCBH_3)(4\text{-phpy})]_2(\mu\text{-bpypz})_2]\}$. Adapted from Ref. [11]. Reproduced by permission of the Royal Society of Chemistry.

methyl-2′-pyridyl)benzimidazolyl)]methane) was investigated by Williams and co-workers in solution [10a]. The thermal spin conversion was interpreted as a two-step spin equilibrium characterized by two distinct characteristic temperatures. The thermodynamic analysis of the data supports the idea that the two steps in solution stem from the occurrence of a negative cooperativity via a ligand-mediated interaction between the two iron sites, which stabilizes the LS–HS state. More recently Hannon and co-workers have also investigated the triple helicate dinuclear SCO Fe(II) system $\{[Fe_2(L)_3](X)_4\}$ (L = N-(4-{4-[(E)-1-(1H-5-imidazolyl)methylideneamino]benzyl}phenyl)-lH-4-imidazolylmethanimine; X = PF_6^-, BF_4^-, ClO_4^-) [10b]. Temperature dependent magnetic susceptibility measurements show that the three salts display incomplete spin conversions. In the case of the X = ClO_4^- around 50% of iron(II) ions exhibit a continuous spin transition between 225 K and 70 K. The cations in the three structures are very similar, each iron atom presents a six coordinate pseudo-octahedral coordination sphere bound to three imidazoline units from three different ligand strands. The ligands bind the two metals and wrap around the metal–metal axis leading to the helical structure; both enantiomers are present in the crystal. Unfortunately, the crystal structures of the three compounds were only investigated at 180 K. In the case of X = ClO_4^- this corresponds to a temperature located just in the middle of the 50% spin transition. These data suggest that one site is HS, average bond length Fe(2)–N = 2.140(11) Å, meanwhile the other site is nearly LS, average bond distance Fe(1)–N = 2.060(11) Å.

Kaizaki's group has reported the dinuclear complex $\{[Fe(NCBH_3)(4\text{-phpy})]_2(\mu\text{-bpypz})_2]\}$ (Fig. 5) [11]. In this centrosymmetric dinuclear unit the iron(II) atom exhibits an octahedral coordination sphere defined by two bpypz ligands, one 4-phpy ligand and one $NCBH_3^-$ coordinating anion. Interestingly, the two-step SCO exhibited by this complex has been found to proceed through a 1:1 mixture of HS–HS and LS–LS spin states, which define the plateau (Fig. 5). X-ray crystal determinations have been performed at 296 K, 200 K (at the plateau) and 100 K. At the plateau, the unit cell doubles in size as both HS–HS and LS–LS species become crystallographically independent. The average bond length is Fe–N = 2.116 Å and Fe–N = 2.005 Å for the HS–HS and LS–LS dimers, respectively. Kaizaki and co-workers have also reported the tightly related compound $\{[Fe(NCS)(\mu\text{-bpypz})]_2(\mu\text{-4,4′-bipy})\}\cdot$MeOH. Utilization of 4,4′-bipy instead of 4-phpy allowed the synthesis of a one-dimensional system made up of dinuclear SCO species. LIESST experiments on this compound illustrate the coexistence of SCO and anti-ferromagnetic interaction in the same compound [12].

A series of compounds of general formula $\{[Fe(NCX)(L)]_2(\mu\text{-bpypz})_2]\}$ (L = py, substituted pyridines (py-X = 4-Mepy, 4-Me_2Npy, 3-Mepy, 3-Clpy, 3-Brpy), 4,4′-bipy, 4-phpy and X = BH_3, S) have been characterized by the same group [13a]. All these complexes undergo spin transition through a direct LS–LS ↔ HS–HS process without intermediate plateau, $T_{1/2}$ being located between 100 K and 200 K. Some of these results were confirmed and extended later by Schneider et al. [13b], but interestingly single crystals of $\{[Fe(NCS)(py)]_2(\mu\text{-bpypz})_2]\}$ showed no spin crossover nor did its triazolate analogue $\{[Fe(NCS)(py)]_2(\mu\text{-bpytz})_2]\}$. Among others, one of the dinuclear systems characterized by X-ray diffraction at temperatures above and below T_c is the complex $\{[Fe(NCBH_3)(py)]_2(\mu\text{-bpypz})_2]\}$ ($T_c \approx 200$ K). The average bond distances of the low-spin form (100 K), in the range 1.94–2.08 Å, are shorter than those (2.10–2.26 Å) in the HS form (296 K). A similar SCO behavior as described above was reported for the complex $\{[(pypzH)(NCSe)Fe(\mu\text{-pypz})_2Fe(pypzH)(NCSe)]\}\cdot 2H_2O$ despite in this case the LS–LS ↔ HS–HS transformation is sharper and takes place at higher temperatures ($T_{1/2}$ = 225 K) (Fig. 6) [14]. Crystal structure determinations were carried out at 123 K and 298 K. The average Fe–N distance at 123 K is 1.995(5) Å increasing to 2.181(7) Å at 298 K. Note that the first observation of a direct spin transition process LS–LS ↔ HS–HS was reported for the structurally uncharacterized bpym-bridged complex $\{[Fe(dpa)(NCS)_2]_2bpym\}$ [15].

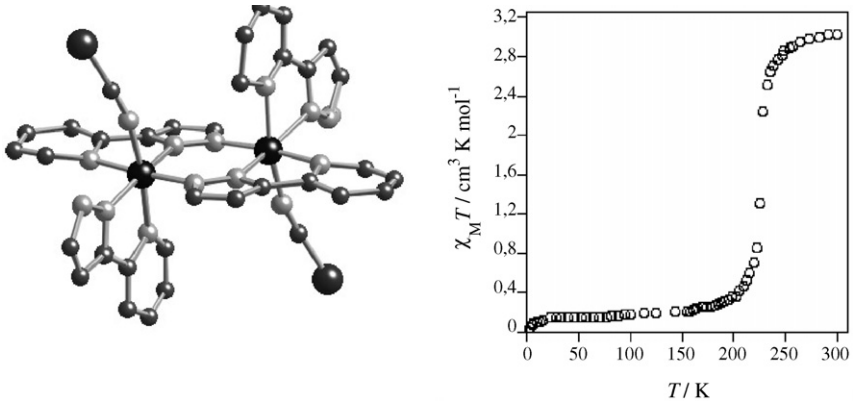

Fig. 6. Molecular structure and magnetic properties of the complex $\{[(pypzH)(NCSe)Fe(\mu\text{-}pypz)_2Fe(pypzH)(NCSe)]\}\cdot 2H_2O$. Adapted from Ref. [14]. Reproduced by permission of the Royal Society of Chemistry.

During the preparation of this review a new dinuclear iron(II) spin crossover compound was reported by Kepert and Murray and co-workers. This compound comprises a new pyridyl bridging ligand, 2,5-di(2′,2″-dipyridylamino)pyridine (DDPP) and has the formula $[Fe_2(DDPP)_2(NCS)4]\cdot 4CH_2Cl_2$. It undergoes a two-step full spin transition. Structural analysis at each of the three plateau temperatures revealed a dinuclear molecule with spin states HS–HS, LS–HS and LS–LS for the two centers. This is the first time that resolution of the metal centers in a LS–HS ordered state has been achieved in a dinuclear iron(II) spin crossover compound [16].

2. Photophysics in dinuclear spin crossover compounds

SCO phenomena between LS and HS states in coordination complexes are of current interest because the spin state can be controlled by several external stimuli such as temperature, pressure, magnetic field and light irradiation. In this context, photo-induced effects in SCO complexes have been studied extensively. A photo-induced technique for the study of SCO in Fe(II) complexes was first reported by McGarvey and Lawthers in 1982 in a paper describing the use of a pulsed laser to perturb the equilibrium between the singlet (^{1}A) and quintet (^{5}T) states in several Fe(II) complexes in solution [17a]. Then, in 1984, Decurtins et al. discovered that the SCO compound $[Fe(ptz)_6](BF_4)_2$ could be converted in the solid state from the LS state to the HS state by irradiating it with green light at liquid helium temperatures [17b]. This phenomenon was named light induced excited spin state trapping. Just after this observation, Hauser observed the reverse-LIESST effect, in which the HS state generated by LIESST effect could be converted inversely back to the original LS state with red light irradiation [18]. Later, several SCO materials were explored and the thermal stability as well as the dynamical aspects of the LIESST effect were rapidly clarified. In the last decade, the possibility of a phase transition under light irradiation has been discussed from the non-equilibrium phase transition point of view. In this line, local symmetry lowering in the LIESST state was pointed out by a series of studies on the compound $[Fe(2\text{-}pic)_3]Cl_2EtOH$ [19].

Until the late 1990s, the LIESST effect had only been investigated on mononuclear species. It was a quite interesting problem how the LIESST effect could appear in dinuclear SCO compounds. Although the appearance of the intermediate LS–HS state in dinuclear compounds is accounted for by the interplay between inter- and intra-molecular elastic interactions, it is nontrivial to predict the nature (HS–HS or HS–LS) of the photo-induced state. In 1999, Létard et al. observed, for the first time, the LIESST effect in the dinuclear SCO compound $\{[Fe(bt)(NCS)_2]_2bpym\}$ and they assigned the photo-induced phase as the HS–HS state [20]. Later, it was confirmed by Mössbauer spectroscopy [2,3,21] and vibrational spectroscopy [22] that the photo-induced state, obtained by a green or red laser, is truly the HS–HS state. LIESST effects were observed in other members of the $\{[Fe(L)(NCX)_2]_2bpym\}$ dinuclear family, where L is bpym or bt and X = S or Se [22,23]. Dynamical properties were also investigated and discussed in connection with a synergy between intra- and inter-molecular cooperative interactions. This synergy leads not only to the plateau region in the thermal phase transition (LS–HS state) but also to a cascade relaxation process from the photo-generated HS–HS state to the LS–LS state via the LS–HS state. Most recently, Ould Moussa et al. discovered a selective photo-switching to the HS–HS state (647.1 nm and 785 nm) and to the LS–HS state (1342 nm) in $\{[Fe(bt)(NCS)_2]_2bpym\}$ [24,25]. In addition, a reverse-LIESST process was discovered from the photo-induced HS–HS state to the LS–HS state. In this section, the photo-physical properties of the dinuclear SCO complexes are reviewed mainly for the $\{[Fe(L)(NCX)_2]_2bpym\}$ family. Recent results on other dinuclear systems are described shortly.

2.1. LIESST effect from a LS–LS ground state

The first observation of the LIESST effect in dinuclear complexes was made in the complex $\{[Fe(bt)(NCS)_2]_2bpym\}$ [20a]. Two years later another observation of the LIESST effect in a different dinuclear compound was reported [20b]. A singular feature of the $\{[Fe(bt)(NCS)_2]_2bpym\}$ complex is the presence of a clear plateau between two separate spin transitions. The plateau is assigned to the LS–HS intermediate spin state of the molecule and the ground state is the LS–LS state [1]. Fig. 7a shows the interplay between temperature and light irradiation effects on the magnetic properties of $\{[Fe(bt)(NCS)_2]_2bpym\}$.

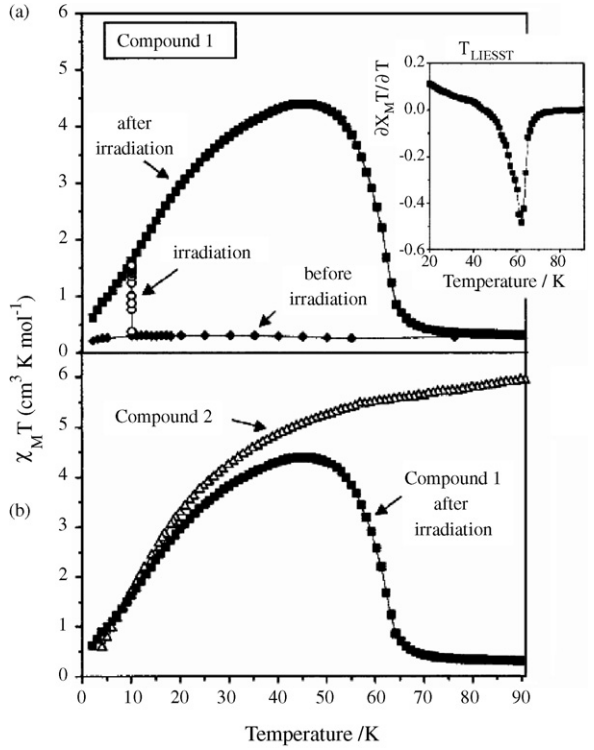

Fig. 7. (a) Temperature dependence of $\chi_M T$ for compound $\{[Fe(bt)(NCS)_2]_2bpym\}$: (♦) data recorded in the cooling mode without irradiation; (◯) data recorded with irradiation for 1 h at 10 K; (■) data recorded in the warming mode after the light irradiation was applied for 1 h, then turned off. The insert graph shows the derivative $\partial(\chi_M T)/\partial T$ plot as a function of the temperature. (b) Comparison of the $\chi_M T$ vs. T curves for $\{[Fe(bpym)(NCS)_2]_2bpym\}$ (△) and $\{[Fe(bt)(NCS)_2]_2bpym\}$ after irradiation (■). Reprinted with permission from Ref. [20a]. Copyright 1999 The American Chemical Society.

At 10 K, before the irradiation, the compound is in the LS–LS ground state. When irradiating with red light (647.1 nm and 676.4 nm), the $\chi_M T$ product increases rapidly and reaches a saturation value around 1.6 cm^3 K mol^{-1}. Without additional irradiation, the temperature dependence was measured. Curiously, the $\chi_M T$ product decreases monotonously with decreasing temperature, and increases considerably with increase of temperature. Above 50 K, the $\chi_M T$ product diminishes rapidly. This photomagnetic behavior strongly indicates that the photo-induced state is the HS–HS state and the temperature dependence may be accounted for by the synergy between the LIESST effect and the intra-molecular anti-ferromagnetic interaction. In fact, the antiferromagnetic coupling between HS states in the dinuclear molecules gives rise to a nonmagnetic S = 0 ground state, which means that $\chi_M T \to 0$ when $T \to 0$. In this respect, the isotropic magnetic exchange taking place in the HS–HS state can be described by the phenomenological spin Hamiltonian:

$$H = -JS_A S_B + g\beta(S_A + S_B)H \quad (1)$$

which leads to the thermal dependence of the $\chi_M T$ product (where χ_M is the magnetic susceptibility and T is the temperature):

$$\chi_M T = \left(\frac{Ng^2\beta^2}{3k_B}\right) \frac{6e^{J/k_BT} + 30e^{3J/k_BT} + 84e^{6J/k_BT} + 180e^{10J/k_BT}}{1 + 3e^{J/k_BT} + 5e^{3J/k_BT} + 7e^{6J/k_BT} + 9e^{10J/k_BT}} \quad (2)$$

with $J = -4.1\,cm^{-1}$ and $g = 2.13$ that predicts an $S = 0$ ground and the $S = 1$, 2, 3, 4 low-lying excited spin levels. This formula reproduces the temperature dependence of the $\chi_M T$ product of the photo-induced metastable phase quite nicely. The strong temperature dependence of the $\chi_M T$ product can therefore be explained by the successive thermal population of the low-lying excited spin levels in the HS–HS state. Such temperature dependence has already been observed in the complex $\{[Fe(bpym)(NCS)_2]_2bpym\}$, in which the HS–HS state is stable in the whole temperature range as a ground state. Comparison of the two systems (Fig. 7b) clearly indicates that the photo-generated state is the HS–HS state. More recently, photo-generation of the HS–HS state in $\{[Fe(bt)(NCS)_2]_2bpym\}$ was also confirmed by Mössbauer spectroscopy under magnetic field after green light irradiation (514.5 nm) [21].

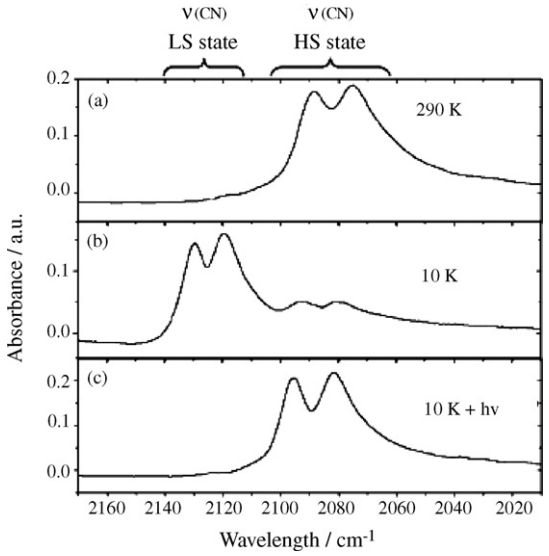

Fig. 8. Infrared spectra of compound $\{[Fe(bt)(NCS)_2]_2bpym\}$ in a KBr disk recorded at: (a) 290 K, (b) 10 K, and (c) 10 K after 1 h of light irradiation. Ref. [22]. Reproduced by permission of the Royal Society of Chemistry.

Generation of the HS–HS state was confirmed by vibrational spectroscopy as well [22,24]. In the case of $\{[Fe(bt)(NCS)_2]_2bpym\}$, the interest in recording vibrational spectra resides in the fact that in the HS–HS and LS–LS states the molecule is centrosymmetric, while the inversion symmetry must be broken if HS–LS units are formed, leading to a drastic change of vibrational spectra. Chastanet et al. investigated the temperature dependence of FTIR spectra of the $\{[Fe(bt)(NCS)_2]_2bpym\}$ compound in detail [22]. Fig. 8a and b shows the CN stretching bands for the HS–HS (290 K) and the LS–LS (10 K) states, respectively. The CN stretching modes change their frequency from the HS–HS state to the LS–LS state so sensitively that one can use these bands as a signature of the spin states. The spectrum after 1 h irradiation with 640 nm light

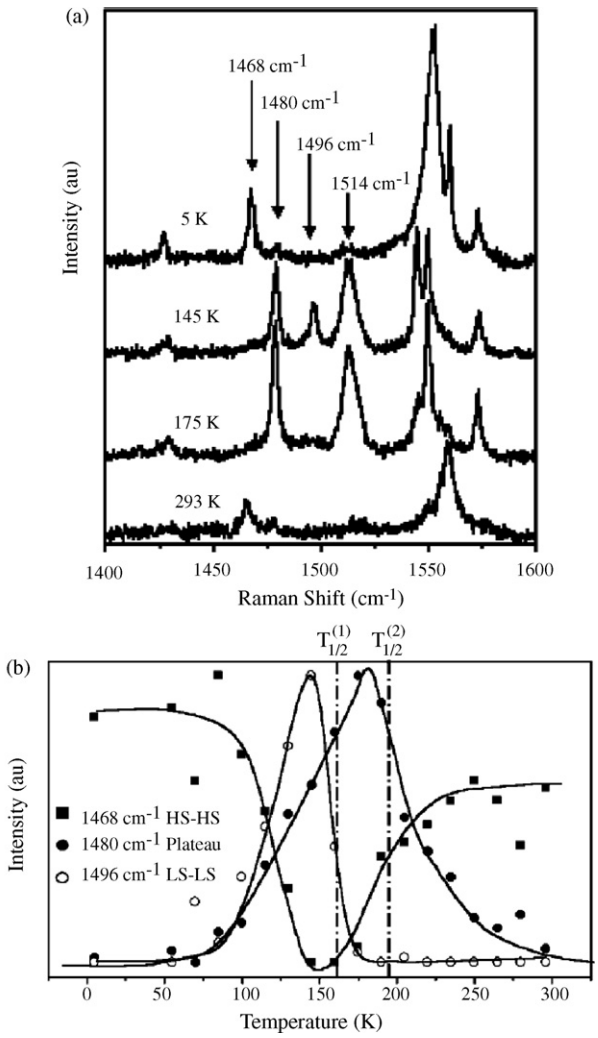

Fig. 9. (a) Selected Raman spectra of the $\{[Fe(bt)(NCS)_2]_2bpym\}$ excited at 647.1 nm, measured at 293 K (HS–HS), 175 K (plateau), 145 K (LS–LS) and 5 K (PIP). (Spectra are represented on different intensity scales for a better clarity.) (b) Temperature dependence of the normalized Raman intensity at 1496 cm^{-1}, 1480 cm^{-1} and 1468 cm^{-1}, characteristic of the LS–LS, plateau and HS–HS regions, respectively. (Lines are inserted to guide the eye.) Reprinted with permission from Ref. [24]. Copyright 2005 the American Physical Society.

at 10 K (Fig. 8c) clearly indicates that the photo-induced state is the HS–HS state.

Raman scattering experiments also support these observations [24,25]. Fig. 9a shows Raman spectra of $\{[Fe(bt)(NCS)_2]_2bpym\}$ recorded between 5 K and 293 K using the 647.1 nm laser line. The spectral region (1400–1600 nm^{-1}) can be assigned to ring deformation and inter-ring stretching vibrations of the bpym ligand. The high temperature (293 K) spectrum corresponds chiefly to the HS–HS state. The spectrum recorded at 175 K (i.e. between $T_{1/2}^{(1)}$ and $T_{1/2}^{(2)}$ in the plateau region) is different in many features both from the HS–HS spectra and from spectra recorded below $T_{1/2}^{(1)}$ at 145 K (LS–LS). For example, inter-ring stretching frequencies at 1468 cm^{-1}, 1496 cm^{-1}, and 1480 cm^{-1} can be assigned to the HS–HS, the LS–LS, and the plateau region, respectively. To better illustrate these assignments, the normalized intensity of selected Raman modes is plotted as a function of temperature in Fig. 9(b), revealing a clear correspondence with the two-step magnetic susceptibility curve. These spectral changes were found to be reversible and reproducible over several cycles. Moreover, the thermal behavior of the ring deformation modes around 1545–1565 cm^{-1} showed similar two-step behavior. The observation of three distinct Raman spectra in correlation with the magnetic behavior confirms and completes the results by Ksenofontov et al. in which the signature of the three spin-pair states was clearly established comparing the Mössbauer spectra in a magnetic field of 5 T before and after LIESST effect at 4 K [2,3,21]. The onset of the photoconversion of the LS Fe(II) ions starts around 145 K and the formation of the photo-induced spin state is complete around 90 K. The spectrum of the photo-induced state differs clearly from the HS–LS and LS–LS spectra and corresponds well to that of the high temperature phase (HS–HS).

Investigation of the dynamics of the generation and relaxation of metastable spin states also appears to be an important issue. A very interesting question concerns the existence of the intermediate mixed LS–HS pair along the photo-excitation process [22]. Fig. 10(a) displays the time dependence of the $\chi_M T$ product expected at 10 K for an indirect LS–LS → LS–HS → HS–HS population (full line) and for a direct LS–LS → HS–HS population (dashed line). In the indirect case, the calculation was carried out on the assumption that the transition rate of the first LS–LS → LS–HS process is larger than that of the second LS–HS → HS–HS process. The difference is linked to the magnetic response of the LS–HS state which is higher at low temperature than that of the HS–HS state. Experimentally, the photo-excitation process was recorded in $\{[Fe(bt)(NCS)_2]_2bpym\}$ at 10 K with red light irradiation (647.1 nm and 676.4 nm) [22]. The time development of the $\chi_M T$ product always increased to the saturation limit corresponding to the expected value for the antiferromagnetic HS–HS pair (similar consideration on the antiferromagnetic HS–HS coupling will appear in the next section). From this result, Chastanet et al. claimed that it seems reasonable to conclude that the photo-excitation of the LS–LS pair would occur through a direct process to the HS–HS state with a quantum yield 2 under red light irradiation. However, there still remains an alternative explanation for the result in Fig. 10b. In fact the generation curve may become a dashed line in Fig. 10a if the system changes via the indirect process (LS–LS → LS–HS → HS–HS) with a much larger transition rate in the latter LS–HS → HS–HS process than that in the former LS–LS → LS–HS process, which is in the counter-limit of the assumption used in the calculation for the indirect process (full line in Fig. 10a).

In close connection with the excitation process, it is quite important to understand the interplay between inter- and intra-molecular interactions in the relaxation process as well. In $\{[Fe(bt)(NCS)_2]_2bpym\}$, two relaxation pathways are expected from the HS–HS state. One is a direct relaxation HS–HS → LS–LS and the other is an indirect relaxation HS–HS → LS–HS → LS–LS. Chastanet et al. clarified by photo-magnetic experiments that the direct HS–HS → LS–LS process is negligible and the indirect process is relevant [22].

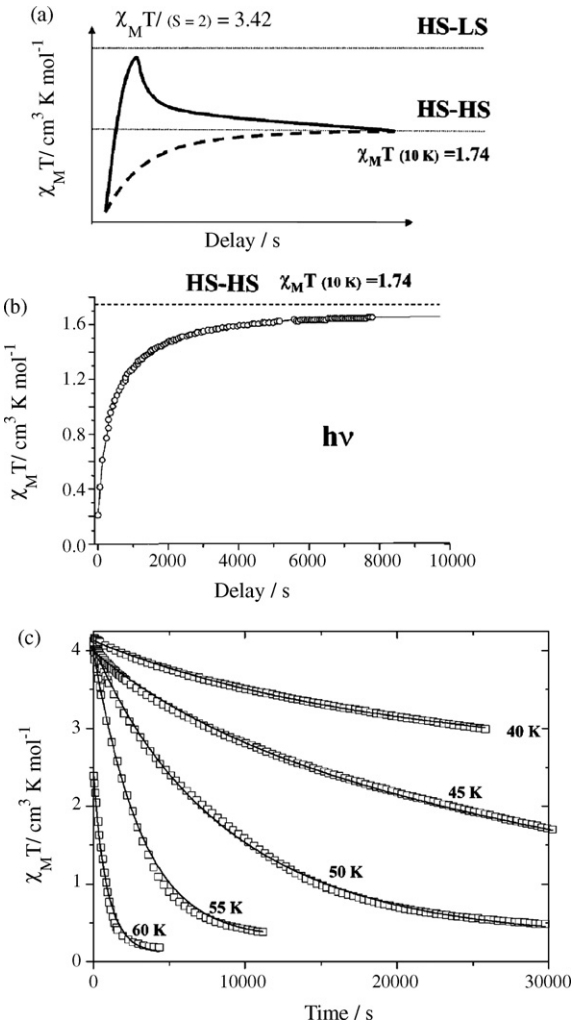

Fig. 10. (a) Schematic view of the expected magnetic behavior at 10 K for a direct LS–LS → HS–HS process (dashed line) and for an indirect LS–LS → LS–HS → HS–HS pathway (full line). (b) Experimental time dependency of the magnetic signal of $\{[Fe(bt)(NCS)_2]_2bpym\}$ recorded at 10 K under light irradiation (λ = 647.1/676.4 nm, 5 mW cm^{-2}). (c) Time dependence of the $\chi_M T$ product recorded in the 40–60 K temperature range. Ref. [22]. Reproduced by permission of the Royal Society of Chemistry.

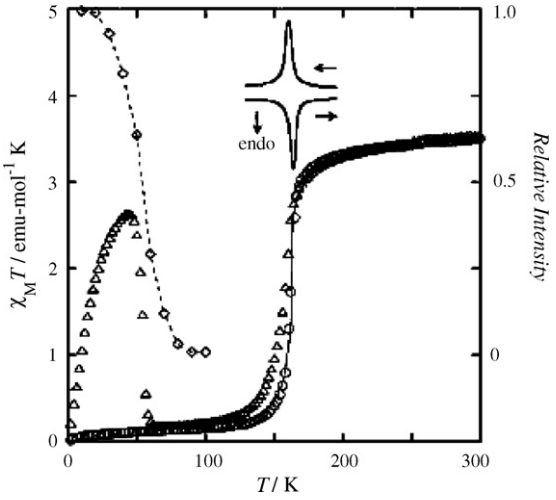

Fig. 11. Temperature dependence of $\chi_M T$ (circle), Raman spectral intensity (lozenge), DSC traces (solid lines), and LIESST (triangle) in $[\{Fe^{II}_2(NCS)_2(\mu\text{-bpypz})_2\}(\mu\text{-4,4}'\text{-bpy})]\cdot MeOH$. A thin solid line indicates the least-squares fitting of the magnetic susceptibility using the regular solution model. Ref. [12]. Reproduced by permission of the Royal Society of Chemistry.

These authors observed the temperature dependent relaxation of the $\chi_M T$ product. After switching off the red light irradiation to obtain the HS–HS state at saturation level, below 18 K, an initial increase of the $\chi_M T$ product was observed, whereas above 18 K only a monotonous decrease was confirmed as shown in Fig. 10c. These results were well reproduced by a simple kinetic model considering a cascade relaxation process HS–HS → LS–HS → LS–LS as shown by solid lines in Fig. 10c. The formation of the LS–HS intermediate state during the relaxation process was also confirmed by Ksenofontov et al. and Gaspar et al. from Mössbauer spectroscopy [2,21]. To understand further the interplay between intra- and inter-molecular interactions, it is necessary to carry out time-resolved measurements using not only magnetic methods but also vibrational spectroscopy and X-ray diffraction.

LIESST effects have been discovered in other dinuclear compounds as well. Ksenofontov et al. observed the LIESST effect by Mössbauer spectroscopy in the $\{[Fe(phdia)(NCS)_2]_2phdia\}$ dinuclear SCO system whose magnetic properties are similar to that of the $\{[Fe(bt)(NCS)_2]_2bpym\}$ compound [2]. However, they observed no HS–HS pairs but LS–HS and LS–LS pairs after illumination with 488 nm light. They also observed that the spin-state after rapid cooling (thermal quenching) is the LS–HS intermediate state. This observation is quite different from the results obtained on the $\{[Fe(L)(NCX)_2]_2bpym\}$ family, suggesting an inherent stability of mixed LS–HS pairs in the $\{[Fe(phdia)(NCS)_2]_2phdia\}$ system. Most recently, Yoneda et al. successfully synthesized a new dinuclear complex based one-dimensional coordination polymer [Fe(NCS)(μ-bpypz)2(μ-4,4′-bpy)] that shows a steep one-step HS–HS to LS–LS transition and they observed a direct photo-conversion from the LS–LS state to the HS–HS state (Fig. 11), suggesting an unstable LS–HS state [12].

2.2. LIESST effect from a LS–HS ground state

Among the $\{[Fe(L)(NCX)_2]_2bpym\}$ family, the $\{[Fe(bpym)(NCSe)_2]_2bpym\}$ compound has the special feature of the LS–HS state being the ground state. At temperatures higher than 120 K the HS–HS state is fully populated. Below 118 K this compound displays a cooperative spin transition, which leads to the formation of the LS–HS state (Fig. 12). The magnetic behavior of $\{[Fe(bpym)(NCSe)_2]_2bpym\}$ can be considered like that of a mononuclear iron(II) complex in the HS state. The decrease of the $\chi_M T$ versus T curve at temperatures lower than 30 K is due to the occurrence of zero-field splitting of the $S = 2$ state as no magnetic exchange can exist in the LS–HS state. The occurrence of an axial zero-field-splitting is expressed by the following Hamiltonian ($S = 2$):

$$H = g\beta HS + D[S_z^2 - (1/3)S(S+1)], \quad (3)$$

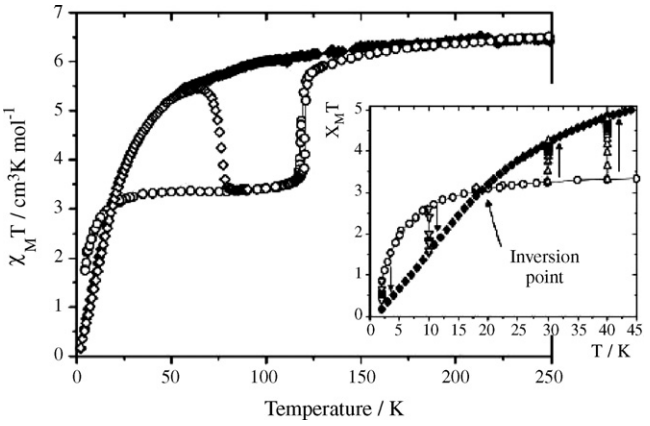

Fig. 12. Temperature dependency of the $\chi_M T$ product for (♦) $\{[Fe(bpym)(NCS)_2]_2bpym\}$ and (◯) $\{[Fe(bpym)(NCSe)_2]_2bpym\}$ without irradiation. The (◊) data correspond to the T(LIESST) measurement, i.e. irradiation time 1 h (λ = 647.1/676.4 nm) then without irradiation the temperature was increased at 0.3 K min^{-1}. Ref. [22]. Reproduced by permission of the Royal Society of Chemistry.

in which all the variables have their usual meaning. The dependence of $\chi_M T$ on T can be expressed as follows:

$$\chi_z T = \frac{2N\beta^2 g_z^2}{k_B}\left[\frac{\exp(x) + 4\exp(-2x)}{\exp(2x) + 2\exp(x) + 2\exp(-2x)}\right] \quad (4)$$

$$\chi_{x,y} T = \frac{2N\beta^2 g_{x,y}^2}{k_B}\frac{1}{3x}\left[\frac{9\exp(2x) - 7\exp(x) - 2\exp(-2x)}{\exp(2x) + 2\exp(x) + 2\exp(-2x)}\right], \quad (5)$$

where $\chi_M T = [(1/3)\chi_z T + (2/3)\chi_{x,y} T]$, $x = D/k_B T$ and D represents the zero-field parameter. This expression simulates perfectly the experimental data with $D = 10\,cm^{-1}$ and $g = 2.22$.

Irradiation at 10 K with red light shows a decrease of the magnetic response from 2.60 cm^3 K mol^{-1} to 1.55 cm^3 K mol^{-1}. This effect is observed at temperatures below ca. 18 K, while an increase of $\chi_M T$ under light irradiation is observed at higher temperatures [22,23]. At first sight, this is a quite surprising behavior. Usually, in a mononuclear Fe(II) SCO compound, the direct LIESST effect results in an increase of the magnetic signal due to the diamagnetic LS response and the paramagnetic HS contribution, while the reverse-LIESST effect induces a decrease of the magnetic signal. In a dinuclear system, however, this situation can be complicated by the presence of intramolecular antiferromagnetic interactions between the two iron(II) metal ions. Clearly, the response of $\{[Fe(bpym)(NCSe)_2]_2bpym\}$ to irradiation with light at temperatures below 18 K does not correspond to a reverse LIESST effect, because the light-induced state has a finite $\chi_M T$ with different temperature dependence from that of the LS–HS state. The temperature dependence of $\chi_M T$ of the photo-induced phase is in good accordance with that of $\{[Fe(bpym)(NCS)_2]_2bpym\}$, where the spin-state is always the HS–HS state (Fig. 12). One can see also the magnetic curves of the ground state and the photo-induced state intersect each other at ca. 18 K (Fig. 12). These features are reproduced excellently by assuming that the light irradiation induces a conversion from a paramagnetic LS–HS state described by Eqs. (3)–(5) to an antiferromagnetically coupled HS–HS state governed by Eqs. (1) and (2). Consequently, light excitation at temperatures above 20 K induces an increase of $\chi_M T$ due to the progressive thermal population of excited $S = 1,2,3,4$ spin levels. For $T < 18$ K these levels depopulate and the $\chi_M T$ values of the photo-generated antiferromagnetic state are smaller than those of the paramagnetic state.

2.3. Selective photo-switching to LS–HS or HS–HS metastable states

A selective photo-switching from the LS–LS ground state to either a metastable paramagnetic HS–LS spin state or to a metastable HS–HS spin state was demonstrated by Ould Moussa et al. in the $\{[Fe(bt)(NCS)_2]_2bpym\}$ system at 10 K under infrared (1342 nm) or red (647 nm) light irradiation, respectively [24,25]. Fig. 13a shows the variation of the $\chi_M T$ product upon cooling in dark as well as the effect of infrared light irradiation and subsequent heating. The data obtained by Létard et al. [20a] using red light irradiation are also plotted in Fig. 13a. This figure reveals the two-step thermal spin conversion upon cooling. At 10 K, the compound is almost quantitatively in the LS–LS state. When irradiating the sample with infrared or red light, the $\chi_M T$ product increases rapidly and reaches a similar value around 1.5 cm^3 mol^{-1} K. As the temperature is slowly increased from 10 K to 100 K without further irradiation, the behavior of the system becomes very different, depending on the wavelength of the preceding photo-excitation. In the case of red light excitation, the $\chi_M T$ product increases markedly up to 44 K, where it reaches a value of 4.4 cm^3 mol^{-1} K. Then, between 55 K and 65 K it drops rapidly to the value measured before photo-excitation. On the contrary, following infrared light irradiation the $\chi_M T$ product increases up to 32 K and reaches only a value of 1.8 cm^3 mol^{-1} K. Subsequently, it drops back more gradually between 40 K and 75 K and rather rapidly above 75 K to the value measured before the photo-excitation. As already described in the previous sections, red light irradiation effects can be explained as the photo-excitation to the HS–HS antiferromagnetically coupled spin states [20a,22]. For 1342 nm irradiation we observe only a very small increase of the $\chi_M T$ product with increasing temperature. A plausible explanation of this behavior is to suppose that light switches the LS–LS state to the paramagnetic ($S = 2$) LS–HS state, which may represent also a metastable point on the potential surface of the system. In this case, the slight increase of the $\chi_M T$ product would correspond to the zero-field splitting, which is expected for the $S = 2$ spin state of the iron(II) ion. Thermal behavior of the photo-excited state (i.e. thermal population of low-lying excited states) indicates the different nature of the photo-induced species generated by the two different excitation wavelengths.

Generation of the LS–HS spin state has been confirmed by Raman scattering under excitation with the 1342 nm laser light [24]. In Fig. 14, temperature dependencies of the intensities of selected Raman lines are displayed. At this excitation wavelength, one can recognize three distinct regions separated by the two phase transition temperatures, $T_{1/2}^{(1)}$ and $T_{1/2}^{(2)}$, corresponding to LS–LS, LS–HS, and HS–HS spin states. The most important

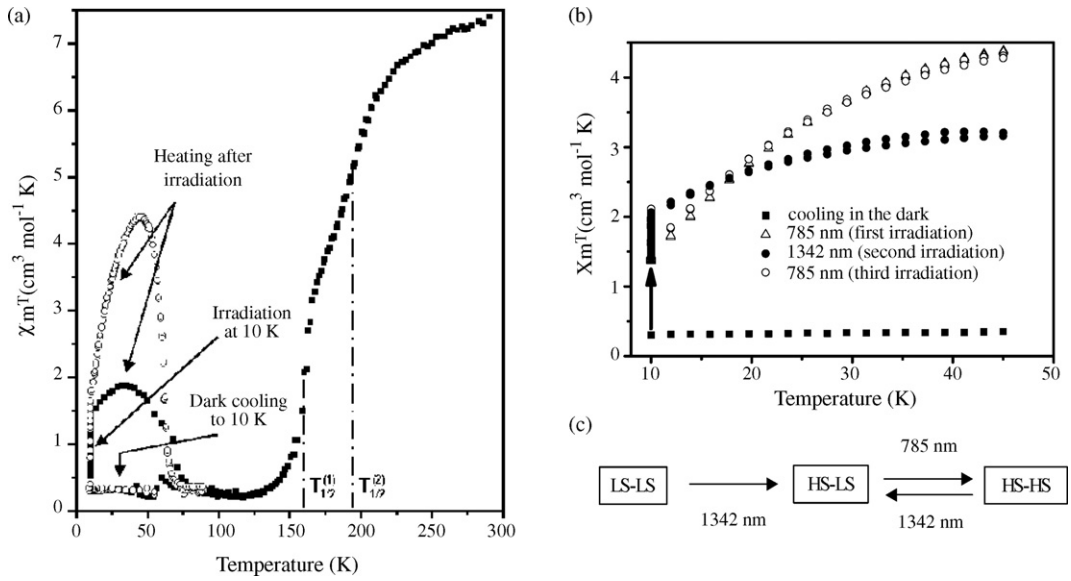

Fig. 13. (a) Temperature dependence of $\chi_M T$ for $\{[Fe(bt)(NCS)_2]_2bpym\}$ recorded in the cooling mode between 293 K and 10 K, followed by 1342 nm light irradiation at 10 K and heating to 100 K (closed symbols). The open symbols are adapted from Ref. [19] and show the same experiment, but using red light (647.1 nm and 676.4 nm). (b) Evolution of the $\chi_M T$ product in $\{[Fe(bt)(NCS)_2]_2bpym\}$ upon successive red, infrared and red light irradiations as a function of the temperature. (c) Schematic representation of the light induced effects. Reprinted with permission from Refs. [24,25a]. Copyrights 2005 and 2007 the American Physical Society.

experimental observation is that in these excitation conditions one can see revival of the LS–HS maker lines and diminishing of the LS–LS maker lines below 75 K. Recently, this behavior was confirmed also by FTIR spectroscopy using CN-stretching bands [25a].

More interestingly, N. Ould Moussa et al. [25a] reported *a cascade excitation* from the photo-induced LS–HS spin state and a *reverse-LIESST effect* from the photo-induced HS–HS spin state to the LS–HS intermediate state by FTIR measurements. When the sample was irradiated with 1342 nm light at 15 K, the LS–HS intermediate state is generated from the LS–LS ground state. In the next step, the sample was irradiated at 15 K by red light (785 nm) leading to a pure HS–HS state. Then, irradiation of this HS–HS state by 1342 nm light led again to the HS–LS spectrum. Temperature dependencies of these two distinct photo-excited spin states shown in Fig. 13b are quite similar to the LIESST effects observed in the $\{[Fe(bpym)(NCSe)_2]_2bpym\}$ system (Fig. 12). These experiments corroborate perfectly the photomagnetic measurements and provide therefore spectroscopic evidence for the photo-induced effects displayed in Fig. 13c.

Selective photo-excitation was also confirmed by X-ray diffraction [25]. Fig. 15 shows the temperature dependence of the unit cell volume, where two anomalies around 200 K and 160 K show the presence of the intermediate LS–HS state. At 23 K, irradiation at 808 nm switches the crystal to the HS–HS state, characterized by a volume of ca. 844 Å^3, whereas the irradiation at 1310 nm leads to the LS–HS state, characterized by a volume of ca. 828 Å^3. In agreement with the magnetic and FTIR data, it is possible to switch in a reversible way between the two photo-induced states (HS–HS and LS–HS) by choosing the appropriate laser excitation wave length. The change of

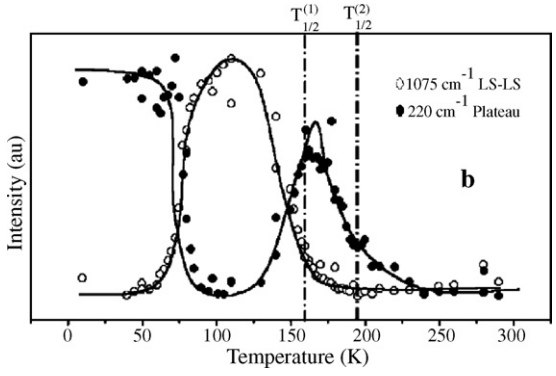

Fig. 14. Temperature dependence of the normalized Raman intensity (excited at 1342 nm) in $\{[Fe(bt)(NCS)_2]_2bpym\}$ at 1075 cm^{-1} and 220 cm^{-1}, characteristic of the LS–LS and plateau regions, respectively. (Lines are inserted to guide the eye.) Reprinted with permission from Ref. [24]. Copyright 2005 the American Physical Society.

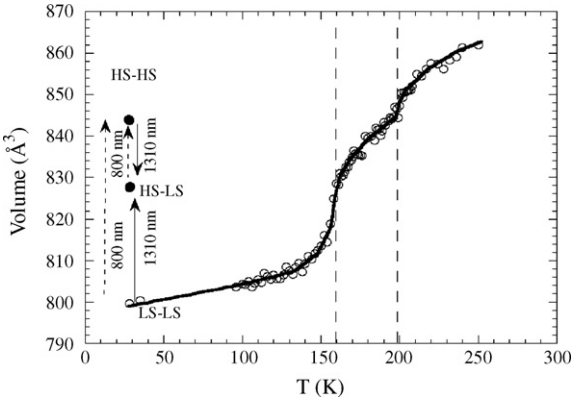

Fig. 15. Temperature dependence of the unit cell volume in $\{[Fe(bt)(NCS)_2]_2bpym\}$ and effect of 1310 nm and 808 nm laser irradiations at 23 K. Reprinted with permission from Ref. [25a]. Copyright 2007 the American Physical Society.

the volume occurs gradually with a gradual shift of the Bragg peaks in the reciprocal space, contrary to what is observed in the case of orihorhombic $[Fe(PM\text{-}BiA)_2(NCS)_2]$ [26] or $[Fe(2\text{-}pic)_3]Cl_2EtOH$ [3c], where a phase separation process takes place. Thus the interactions between the photo-induced molecules are weak and the concentration of photo-doped molecules is homogeneously increased with in the crystal.

The symmetry breaking in the LS–HS state is an important issue that has to be discussed. The formation of photo-induced HS–LS state should involve a spontaneous inversion symmetry breaking [24]. To be exact, for dinuclear SCO compounds, it is a double symmetry breaking at two Néel temperatures, when the HS population of one metallic center becomes different than the HS population of the second center in the network. Curiously, the crystal symmetry of the thermally and photo-induced LS–HS states determined by the X-ray diffraction keeps the same space group $P_{\bar{1}}$ as those in the HS–HS and LS–LS states [25]. A plausible model would be a random distribution of LS–HS and HS–LS pairs in the LS–HS state, which is quite similar to the local symmetry breaking observed in $[Fe(2\text{-}pic)_3]Cl_2{\cdot}EtOH$ [19].

3. Theoretical models for two-step spin crossover in dinuclear compounds

Since the 1970s, several authors have proposed different theoretical approaches for the interpretation of the SCO phenomenon including thermodynamic or microscopic models [27]. The discovery of the two-step character of the SCO in dinuclear compounds was realized only in the 1990s and then its theoretical interpretation followed thus by only a few models.

In 1992 two different approaches were proposed for two-step SCO dinuclear compounds. The first is thermodynamic based on Drikamer's model including an "anti-cooperative" interaction, more exactly a negative interaction in addition to a positive interaction. For a certain balance between positive and negative interactions the SCO may occur in two steps [28,1a]. At the same time another model with a microscopic approach was proposed: the so-called Ising-like model [29], where the interactions of the system have been developed following the Ising magnetic model. In the microscopic model as well, two interactions have been introduced: a ferromagnetic-like interaction (positive) and antiferromagnetic-like interaction (negative). This model has been treated using the mean-field approximation. In 1993, the intra-molecular interaction (negative interaction)was treated exactly while the inter-molecular interaction (positive interaction) was treated in the mean-field approximation [30]. Later, microscopic models were also treated using Monte Carlo simulations [31,32]. In 2004, a novel approach using an atom-phonon coupling model was proposed by J. Nasser et al. [33]. The effects of the short-range interactions were studied leading to a reproduction of some experimental observations with a "plateau" as a function of temperature.

In the Ising-like model framework with exact treatment of the intra-dinuclear interaction and in the case of a uniform inter-dinuclear interaction (ferro-like interaction), the two step character of the SCO is due to a double symmetry breaking of the magnetization of the system as a function of the temperature, leading to a λ-point in the $C_P(T)$ function. In this case, a second order phase transition as a function of the temperature is expected [30].

The dynamics of the SCO phenomenon is of course very exciting in particular for dinuclear systems and more generally in two-step SCO systems. In 2002, an elegant approach was proposed by Y. Ogawa et al. [34] in the case of the mononuclear $[Fe(2\text{-}pic)_3]Cl_2{\cdot}EtOH$, including the vibrational degrees of freedom of the molecules and short- as well as long-range interactions. The magnetic field was a good tool to follow the dynamics of the system using the Ising-like model approach [29,35]. The dynamic properties of two-step SCO were studied in more detail by K. Boukheddaden et al. [36], who introduced in the Ising-like model [29] dynamics using the general formalism of the master-equation introduced by Glauber [37] in which the transition rates obey the Arrhenius law. In this work, the theoretical relaxation curves show some differences to the experimental data. This is certainly due to the mean-field approximation used for the analytical treatment of the model. Some interesting papers where the theoretical approaches of the dynamics are studied out of the mean-field approximation and better adapted for the two-step spin transition can been found in Refs. [38–40].

DFT calculations on dinuclear compounds have been carried out only very recently [4]. Five dinuclear compounds have been analyzed. Three electronic states corresponding to LS–LS, LS–HS and HS–HS configurations were characterized leading to the conclusion that the interactions in the system are mainly elastic rather than weak magnetic interactions (antiferromagnetic $\sim 4\,cm^{-1}$). In addition the enthalpy of the LS–HS state was found lower than the average enthalpy of the LS–LS and HS–HS states in agreement with the two-step spin conversion observed in the system.

4. Concluding remarks

Dinuclear SCO compounds were an exciting idea of Olivier Kahn in order to combine SCO and magnetic coupling within the same molecule. Synergy between these two phenomena is most easily observed at low temperatures where visible and infrared light irradiation may populate long-lived metastable states. Indeed, the photo magnetic properties of these compounds are very singular. However, there remain several unsolved problems concerning the nature and dynamic properties of the LS–HS intermediate state in dinuclear complexes. Further investigations using recently synthesized complexes and time-resolved spectroscopic techniques will lead to a deeper insight of the physics and chemistry of these fascinating molecules.

Acknowledgments

We would like to thank our numerous collaborators, whose contributions have been cited in this review. We thank also for the financial support the Picasso project (Acción Integrada HF2005-0117), European Action COST D35, the Spanish M.E.C. (project CTQ 2004-03456/BQU) and the Grant-in-Aid

for Creative Scientific Research Program of the Ministry of Education, Culture, Sports, Science and Technology of Japan.

References

[1] (a) J.A. Real, H. Bolvin, A. Bousseksou, A. Dworkin, O. Kahn, F. Varret, J. Zarembowitch, J. Am. Chem. Soc. 114 (1992) 4650;
(b) J.A. Real, A.B. Gaspar, M.C. Muñoz, P. Gütlich, V. Ksenofontov, H. Spiering, Top. Curr. Chem. 233 (2004) 167;
(c) A.B. Gaspar, M.C. Muñoz, J.A. Real, J. Mater. Chem. 16 (2006) 2522.

[2] V. Ksenofontov, A.B. Gaspar, S. Reiman, V. Niel, J.A. Real, P. Gütlich, Chem. Eur. J. 10 (2004) 1291.

[3] (a) V. Ksenofontov, H. Spiering, S. Reiman, Y. Garcia, A.B. Gaspar, N. Moliner, J.A. Real, P. Gütlich, Chem. Phys. Lett. 348 (2001) 381;
(b) A.B. Gaspar, V. Ksenofontov, H. Spiering, S. Reiman, J.A. Real, P. Gütlich, Hyperfine Interact. 144/145 (2002) 297;
(c) V. Ksenofontov, H. Spiering, S. Reiman, Y. Garcia, A.B. Gaspar, N. Moliner, J.A. Real, P. Gütlich, Hyperfine Interact. 141/142 (2001) 47.

[4] S. Zein, S.A. Borshch, J. Am. Chem. Soc. 127 (2005) 16197.

[5] N. Ortega-Villar, A.L. Thompson, M.C. Muñoz, V.M. Ugalde-Saldívar, A.E. Goeta, R. Moreno-Esparza, J.A. Real, Chem. Eur. J. 11 (2005) 5721.

[6] M.H. Klingele, B. Moubaraki, J.D. Cashion, K.S. Murray, S. Brooker, Chem. Commun. (2005) 987.

[7] (a) J.A. Real, I. Castro, A. Bousseksou, M. Verdaguer, R. Burriel, M. Castro, J. Linares, F. Varret, Inorg. Chem. 36 (1997) 455;
(b) V. Ksenofontov, A.B. Gaspar, J.A. Real, P. Gütlich, J. Chem. Phys. B 105 (2001) 12266.

[8] M.L. Flay, V. Comte, H. Vahrenkamp, Z. Anorg, Allerg. Chem. 629 (2003) 1147.

[9] M. Nihei, M. Ui, M. Yokota, L. Han, A. Maeda, H. Kishida, H. Okamoto, H. Oshio, Angew. Chem. Int. Ed. 44 (2005) 6484.

[10] (a) S.G. Teller, B. Bocquet, A.F. Williams, Inorg. Chem. 40 (2001) 4818;
(b) F. Tuna, M.R. Lees, G.J. Clarkson, M.J. Hannon, Chem. Eur. J. 10 (2004) 5737.

[11] K. Nakamo, S. Kawata, K. Yoneda, A. Fuyuhiro, T. Yagi, S. Nasu, S. Morimoto, S. Kaizaki, Chem. Commun. (2004) 2892.

[12] K. Yoneda, K. Adachi, S. Hayami, Y. Maeda, M. Katada, A. Fuyuhiro, S. Kawata, S. Kaizaki, Chem. Commun. (2006) 45.

[13] (a) K. Nakano, N. Suemura, K. Yoneda, S. Kawata, S. Kaizaki, Dalton Trans. (2005) 740;
(b) C.J. Schneider, J.D. Cashion, B. Moubaraki, S.M. Neville, S.R. Batten, D.R. Turner, K.S. Murray, Polyhedron 26 (2007) 1764.

[14] B.A. Leita, B. Moubaraki, K. Murray, J.P. Smith, J.D. Cashion, Chem. Commun. (2004) 156.

[15] A.B. Gaspar, V. Ksenofontov, J.A. Real, P. Gütlich, Chem. Phys. Lett. 373 (2003) 385.

[16] J.J. Amoore, C.J. Kepert, J.D. Cashion, B. Moubaraki, S.M. Neville, K.S. Murray, Chem. Eur. J. 12 (2006) 8220.

[17] (a) J.J. McGarvey, I. Lawthers, J. Chem. Soc., Chem. Commun. (1982) 906;
(b) S. Decurtins, P. Gütlich, C.P. Köhler, H. Spiering, A. Hauser, Chem. Phys. Lett. 105 (1984) 1.

[18] A. Hauser, P. Gütlich, H. Spiering, Inorg. Chem. 25 (1986) 4245.

[19] (a) T. Tayagaki, K. Tanaka, Phys. Rev. Lett. 86 (2001) 2886;
(b) T. Tayagaki, K. Tanaka, H. Okamura, Phys. Rev. B 69 (2004) 064104;
(c) N. Huby, L. Guérin, E. Collet, L. Toupet, J.C. Ameline, H. Cailleau, T. Roisnel, T. Tayagaki, K. Tanaka, Phys. Rev. B 69 (2004) 020101(R).

[20] (a) J.-F. Létard, J.A. Real, N. Moliner, A.B. Gaspar, L. Capes, O. Cador, O. Kahn, J. Am. Chem. Soc. 121 (1999) 10630;
(b) N. Suemura, M. Ohama, S. Kaizaki, Chem. Commun. (2001) 1538.

[21] A.B. Gaspar, V. Ksenofontov, S. Reiman, P. Gütlich, H.L. Thompson, A.E. Goeta, M.C. Muñoz, J.A. Real, Chem. Eur. J. 12 (2006) 9289.

[22] G. Chastanet, C. Carbonera, C. Mingotaud, J.-F. Létard, J. Mater. Chem. 14 (2004) 3516.

[23] G. Chastanet, A.B. Gaspar, J.A. Real, J.-F. Létard, Chem. Commun. (2001) 819.

[24] N. Ould Moussa, G. Molnár, S. Bonhommeau, A. Zwick, S. Mouri, K. Tanaka, J.A. Real, A. Bousseksou, Phys. Rev. Lett. 94 (2005) 107205.

[25] (a) N. Ould Moussa, E. Trzop, S. Mouri, S. Zein, G. Molnár, A.B. Gaspar, E. Collet, J.A. Real, S. Borshch, K. Tanaka, H. Cailleau, A. Bousseksou, Phys. Rev. B 75 (2007) 054101;
(b) E. Trzop, M. Buron-Le Cointe, H. Cailleau, L. Toupet, G. Molnár, A. Bousseksou, A.B. Gaspar, J.A. Real, E. Collet, J. Appl. Cryst. 40 (2007) 158.

[26] K. Ichiyanagi, J. Hebert, L. Toupet, H. Cailleau, P. Guionneau, J.-F. Létard, E. Collet, Phys. Rev. B 73 (2006) 060408 (R).

[27] P. Gütlich, H.A. Goodwin, Top. Curr. Chem. 233 (2004) 1.

[28] V. Niel, A.L. Thompson, A.E. Goeta, C. Enachescu, A. Hauser, A. Galet, M.C. Munoz, J.A. Real, Chem. Eur. J. 11 (2005) 2047.

[29] A. Bousseksou, J. Nasser, J. Linares, K. Boukheddaden, F. Varret, J. Phys. I France 2 (1992) 1381.

[30] A. Bousseksou, F. Varret, J. Nasser, J. Phys. I France 3 (1993) 1463.

[31] (a) J. Linares, J. Nasser, K. Boukheddaden, A. Bousseksou, F. Varret, J. Magn. Magn. Mater. 140 (1995) 1507;
(b) J. Linares, J. Nasser, A. Bousseksou, K. Boukheddaden, F. Varret, J. Magn. Magn. Mater. 140 (1995) 1503.

[32] H. Romstedt, A. Hauser, H. Spiering, J. Phys. Chem. Solids 59 (1997) 265.

[33] J.A. Nasser, K. Boukheddaden, J. Linares, Eur. J. Phys. B 39 (2004) 219.

[34] Y. Ogawa, T. Ishikawa, S. Koshihara, K. Boukheddaden, F. Varret, Phys. Rev. B 66 (2002) 073104.

[35] (a) K. Boukheddaden, I. Shteto, B. Hôo, F. Varret, Phys. Rev. B 62 (2000) 14796;
(b) K. Boukheddaden, I. Shteto, B. Hôo, F. Varret, Phys. Rev. B 62 (2000) 14806.

[36] K. Boukheddaden, J. Linares, E. Codjovi, F. Varret, J. Appl. Phys. 93 (2003) 7103.

[37] R.J. Glauber, J. Math. Phys. 4 (1963) 294.

[38] K. Boukheddaden, F. Varret, S. Salunke, J. Linares, E. Codjovi, Phase Transit. 75 (2002) 733.

[39] M. Nishino, K. Boukheddaden, S. Miyashita, F. Varret, Phys. Rev. B 68 (2003) 224402.

[40] M. Nishino, K. Boukheddaden, S. Miyashita, F. Varret, Polyhedron 24 (2005) 2852.